Electronic Supplementary Material (ESI) for Journal of Materials Chemistry A.

Electronic Supplementary Information

The effect of oxygen on the efficiency in planar *p-i-n* metal halide perovskite solar cells with a PEDOT:PSS hole transport layer

Bardo J. Bruijnaers, Eric Schiepers, Christ H. L. Weijtens, Stefan C. J. Meskers, Martijn M. Wienk and René A. J. Janssen

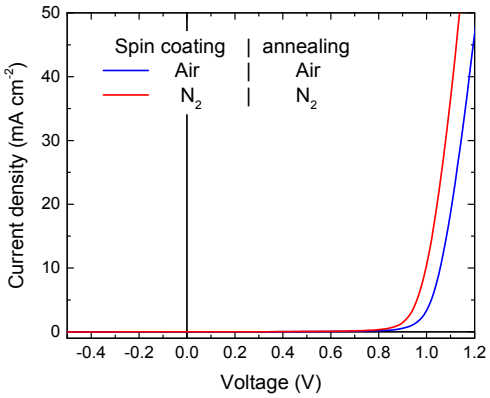

Fig. S1 Dark *J*–*V* characteristics of solar cells processed completely in air (blue) and nitrogen (red) corresponding to the *J*-*V* characteristics in Fig. 1a in the main text.

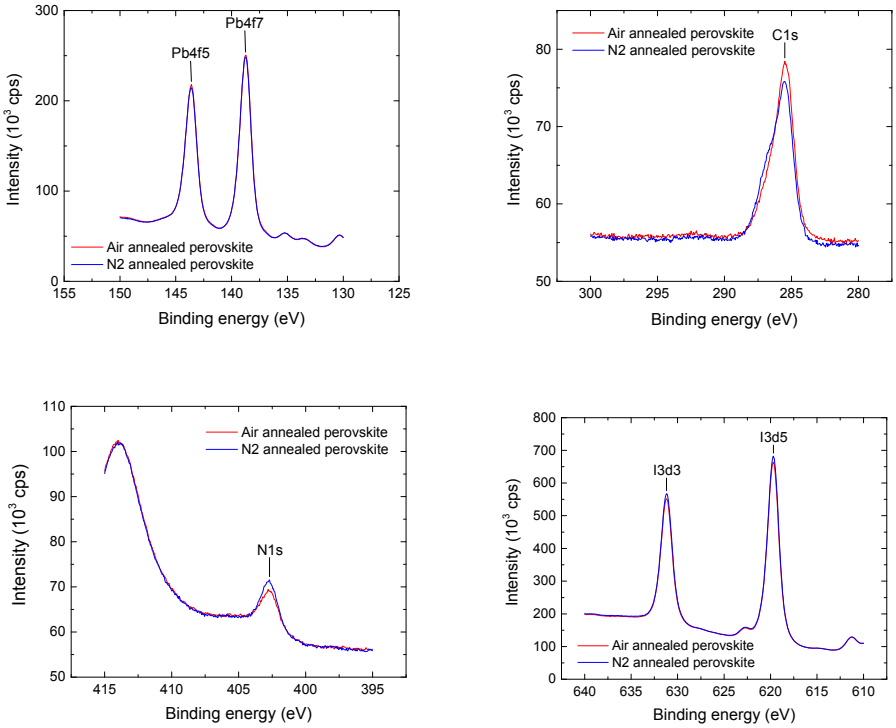

Fig. S2 High resolution XPS spectra for lead (Pb), carbon (C), nitrogen (N) and iodide (I) for perovskite layers annealed in air (red) and nitrogen (blue).

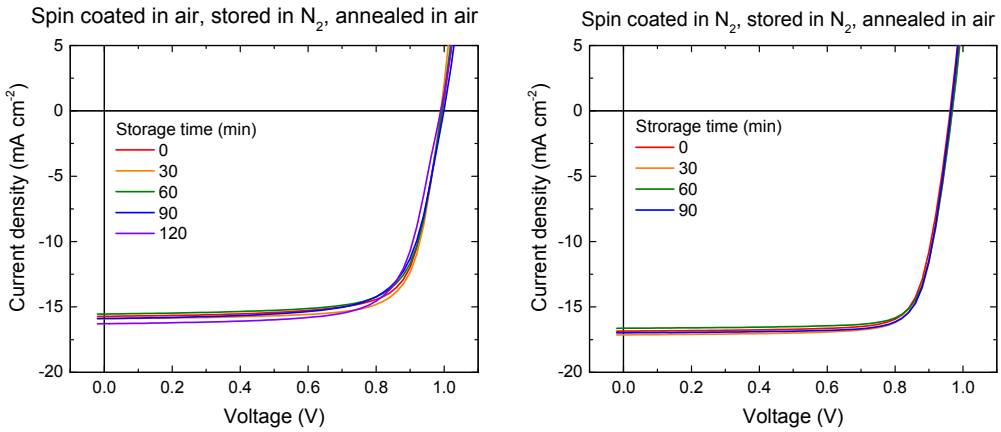

Fig. S3 Stabilized *J*–*V* characteristics of solar cells spin coated in air (left) and nitrogen (right) and stored in a nitrogen atmosphere for 0 – 120 minutes before annealing as indicated in the legend.

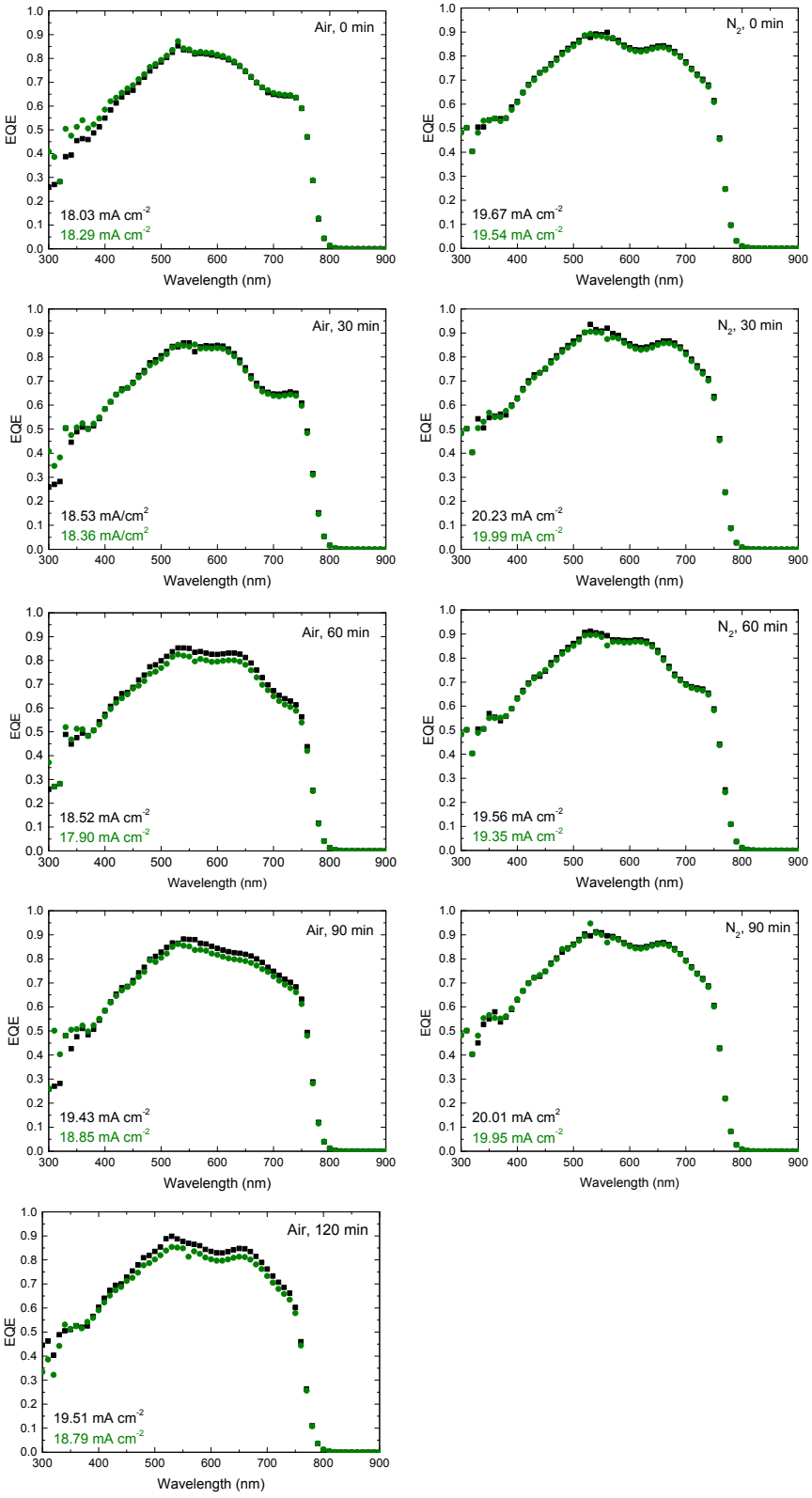

Fig. S4 EQE spectra of solar cells spin coated in air (left) and nitrogen (right) and stored in a nitrogen atmosphere for 0 – 120 minutes before annealing. Black squares depict the EQE under low charge carrier density (i.e. without bias illumination), green circles depict the EQE at a charge carrier density similar to that of the cell under 1-sun light intensity (i.e. with bias illumination). The integrated current density is displayed in the graphs for both measurements.

Room temperature static casting of perovskite layers

The hot casting procedure has proven to be very reliable and reproducible in our lab,[1] it is however a technique that has not found widespread use in other labs for the production of perovskite solar cells. In order to verify that the effects we observe using the hot cast method also appear in solar cells produced using the much more generally used room temperature spin coating, solar cells were also produced using room temperature spin coating (cold casting). For this experiment, the same precursor mixture was used (at a 1.8× higher concentration in order to achieve the optimal perovskite layer thickness) which was spin coated with solution and substrate at room temperature in the regular fashion (solution is deposited before spinning of the substrate is started). Since spin coating this precursor solution at room temperature in air results in rough perovskite layers with many pinholes after annealing, resulting in solar cells with low performance. The cells for this experiment were spin coated in an N_2 atmosphere and annealed in either dry nitrogen or air. SEM images of the layers are shown in Fig. S4.

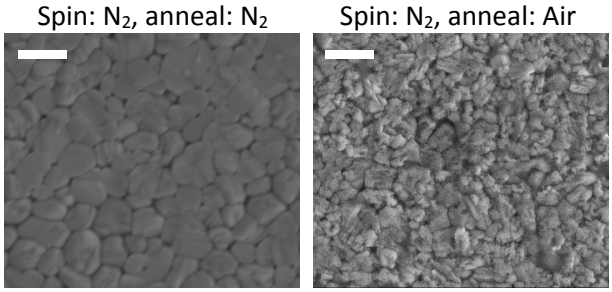

Fig. S5 SEM top view images of perovskite layers spin coated in N_2 using the cold cast method and annealed in N_2 and air as indicated above the images (scale bars are 1µm).

The solar cells produced in this experiment also show a significantly higher J_{SC} and V_{OC} for the cells annealed in air than those annealed in N_2 in the *J*–*V* characteristic (Fig. S5 and Table S1), similar to the hot cast results. Similar to the hot-cast layers, the EQE of the N_2-annealed cells also drops significantly under bias illumination (Fig. S6). This provides proof that the decreases the performance of N_2 annealed perovskite layers is not exclusive to the hot cast procedure.

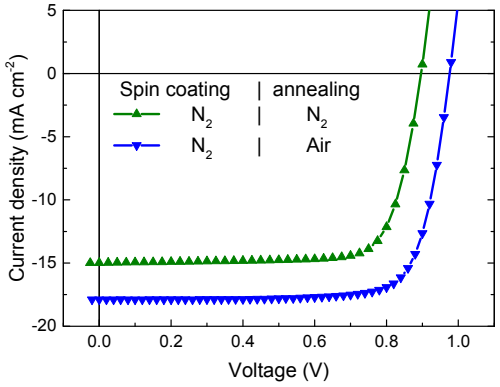

Fig. S6 Stabilized *J-V* characteristics of perovskite solar cells spin coated in N_2 using the cold cast method and annealed in N_2 and air as indicated by the legend.

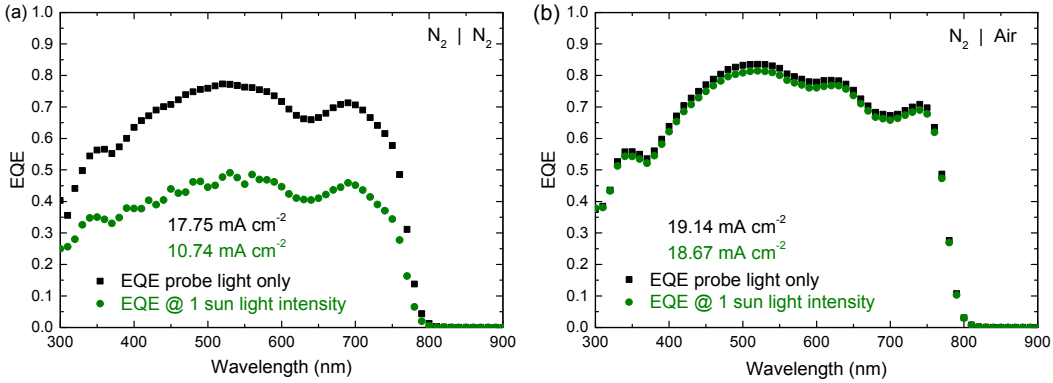

Fig. S7 EQE of perovskite solar cells with a perovskite layer spin coated in N_2 using the cold cast method and annealed in N_2 (a) and air (b).

Table S1 Photovoltaic parameters of perovskite solar cells spin coated in N_2 using the cold cast method and annealed in N_2 or air.

Spin coating atmosphere	Annealing atmosphere	Perovskite thickness (nm)	$J_{SC,\ J\text{-}V}$ (mA cm^{-2})	$J_{SC,\ SR\ @\ 1sun}$ (mA cm^{-2})	V_{OC} (V)	FF	PCE (%)
N_2	N_2	475	15.0	10.7	0.90	0.76	7.5
N_2	Air	362	17.9	18.7	0.98	0.78	14.3

Room temperature and low temperature photoluminescence

Photoluminescence (PL) measurements on perovskite layers deposited on top of a non-quenching poly(4-styrene sulfonic acid) (PSSH) layer and annealed in nitrogen and air show that the peak position and shape of the emission spectrum is similar for both samples (Fig. S7a). Illumination intensity dependent measurements also show no significant difference between the two perovskite layers at both low and high illumination intensities (Fig. S7b). A clear change from a slope of 1.5 for lower light intensities to a slope of 1 for high light intensities in a log-log plot is visible. This indicates a transition from dominant trap assisted (SRH) recombination (slope = 1.5) to dominant band-to band (free carrier) recombination (slope = 1) at a charge carrier density of about 1 sun AM 1.5 illumination intensity.[2–5] The PL spectrum does not change with increasing illumination intensity.

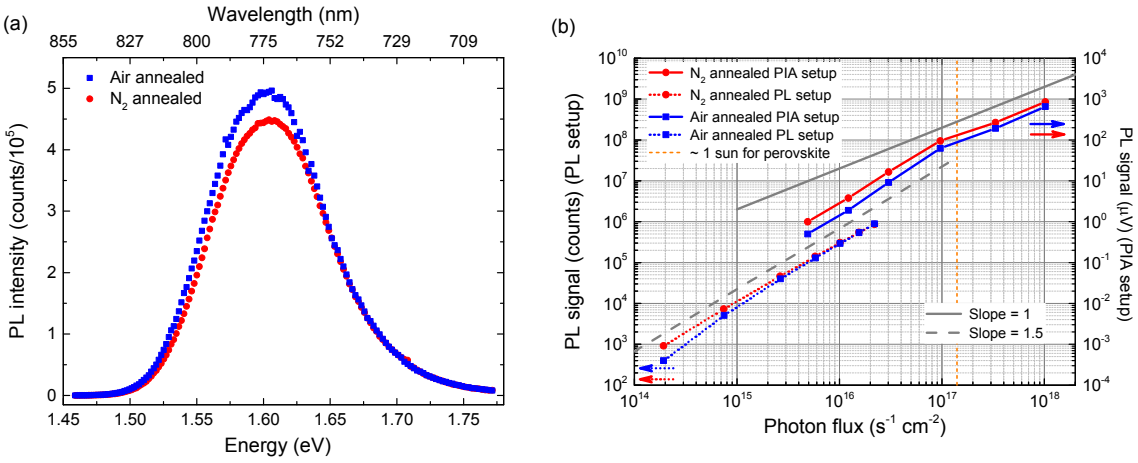

Fig. S8 (a) Photoluminescence spectra at room temperature of perovskite layers annealed in air (blue solid squares) and nitrogen (red solid circles). (b) Illumination intensity dependent photoluminescence of perovskite layers annealed in air (blue solid squares) and nitrogen (red solid circles) at room temperature measured in two different setups to cover a larger photon flux range including illumination intensities that generate charge carrier densities ≥ 1 sun AM1.5 illumination intensity. Lines with slopes of 1 and 3/2 (in a log-log plot) indicating different recombination mechanisms are also added. The wavelengths measured were the peak maxima in both setups.

Upon cooling to 70 K, the peak position and shape changes similarly for both samples through the range of temperatures (Fig. S8) and similar as reported in literature.[2] The spectra recorded at 70 K for air- and N_2-annealed layers are shown in Fig. 5a in the main text and are very similar, also at different illumination intensities. In addition a weak defect emission at 0.96 eV (~1300 nm)[6] is observed (Fig. S9). The 0.96 eV band shows higher intensity for the N_2-annealed sample.

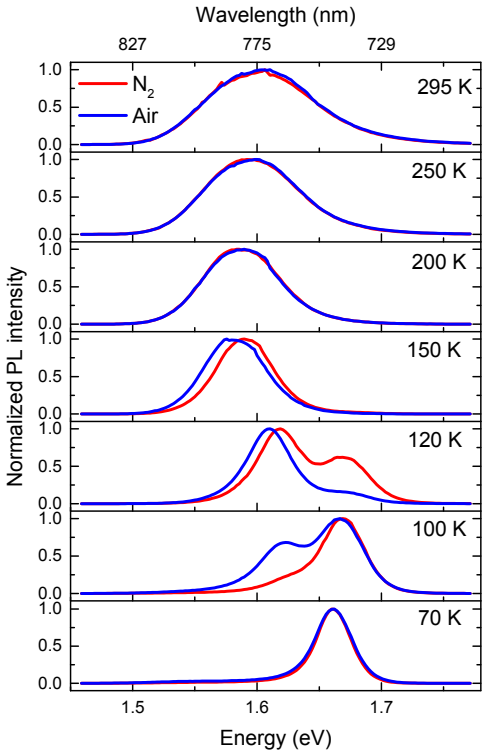

Fig. S9 Normalized photoluminescence spectra of perovskite layers annealed in nitrogen (red) and air (blue) through a range of temperatures while cooling down from room temperature to 70 K.

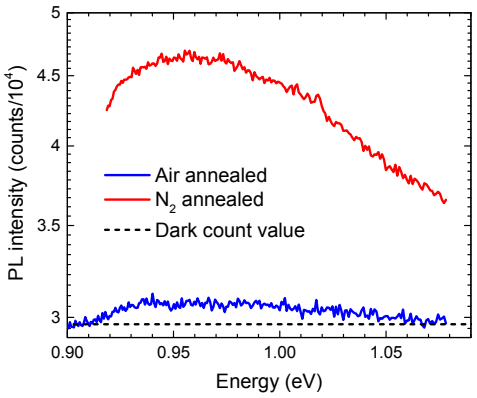

Fig. S10 Low-energy region of the photoluminescence spectra recorded at 70 K of perovskite layers annealed in air (blue) and nitrogen (red) at high (dash) and low (solid) illumination intensities.

The illumination intensity dependent photoluminescence at 70 K of the main emission peak (Fig. S10a) looks very similar to the one measured at room temperature (Fig. S7b low illumination intensity) again with a slope of 1.5 indicating trap assisted recombination. The slope is nearly 1 for both defect emissions (Fig. S10b and S10c) and there is again no significant difference caused by the different annealing atmospheres. All these photoluminescence measurements combined indicate that the bulk physical properties of the layers are very similar and the only small difference that can be found is in the low energy defect.

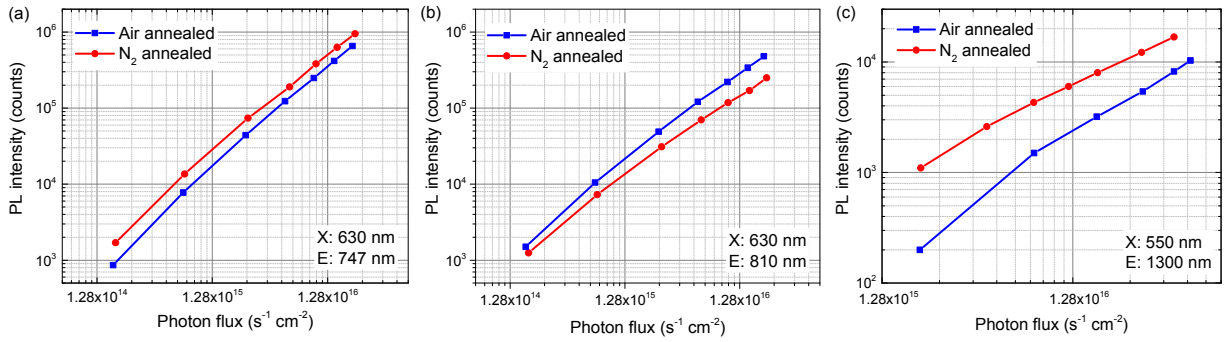

Fig. S11 Illumination intensity dependent photoluminescence at 70 K of perovskite layers annealed in air (blue) and nitrogen (red) at three different wavelengths. Excitation (X) and emission (E) wavelengths are displayed in each graph. For the 1300 nm graph, the dark count was subtracted.

Room temperature and low temperature electroluminescence

Fig. S11 shows the data recorded for the EQ-ELE experiments shown in Fig. 5b in the main text. It can be seen that the current-voltage characteristics are similar (except for the ~0.1 V shifted onset, see Fig. S1) and that between 1.0 and 1.3 V, the light emitted by the air-annealed device is higher than for the N_2-annealed device.

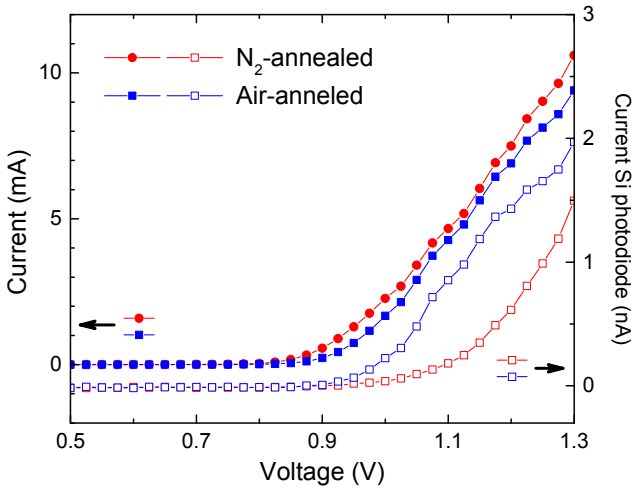

Fig. S12 Current-voltage characteristics of perovskite devices (solid symbols) and the simultaneously recorded photocurrent of a silicon photodiode placed on top.

In electroluminescence (EL) measurements at different voltages at room temperature and 70 K, again no significant differences can be found in peak shape and position (Fig. S12). Due to the high sensitivity of the measured intensities to the alignment of the sample inside the cryostat in our setup, we are not able to make a firm conclusion about any differences in intensities that may be related to improvement of contacts by air-annealing. We did notice, however, that especially at lower

temperatures, the current running through the air-annealed samples was significantly lower than for the N_2-annealed samples for similar light intensities.

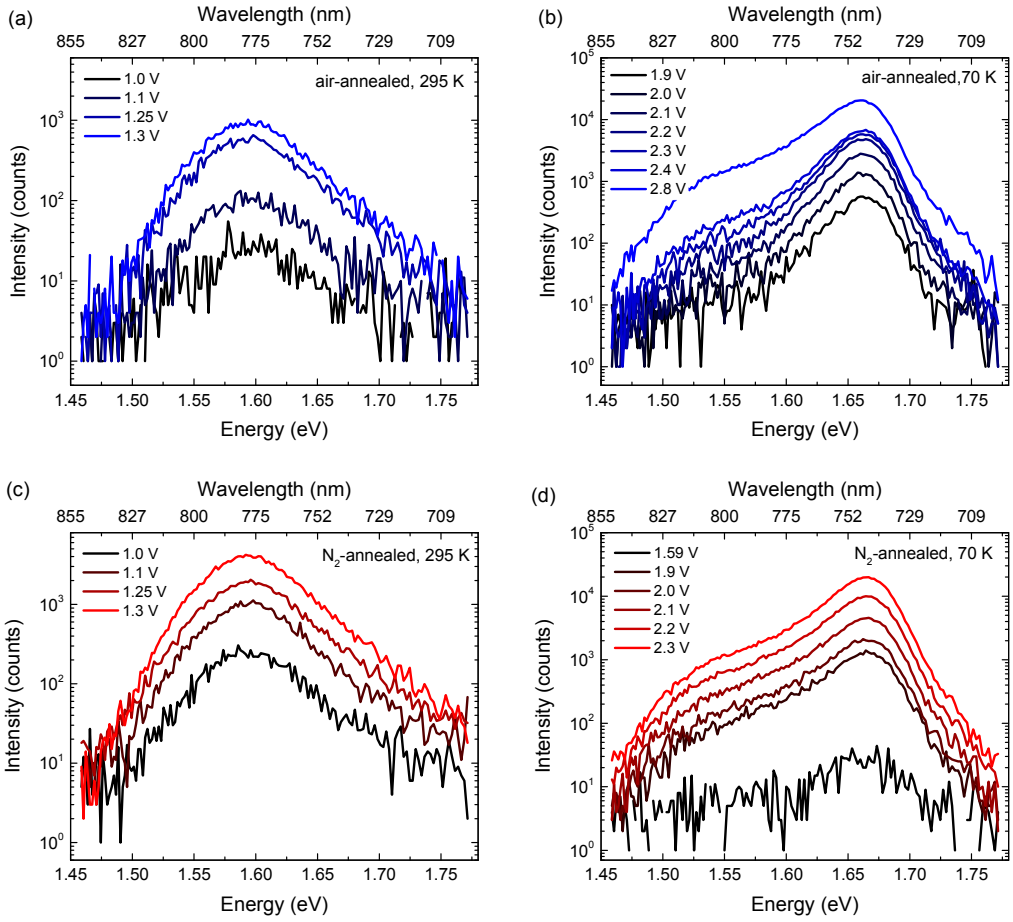

Fig. S13 Electroluminescence (EL) spectra recorded at 295 K (a, c) and 70 K (b, d) at different voltages for air (a, b)) and N_2 (c, d) annealed samples.

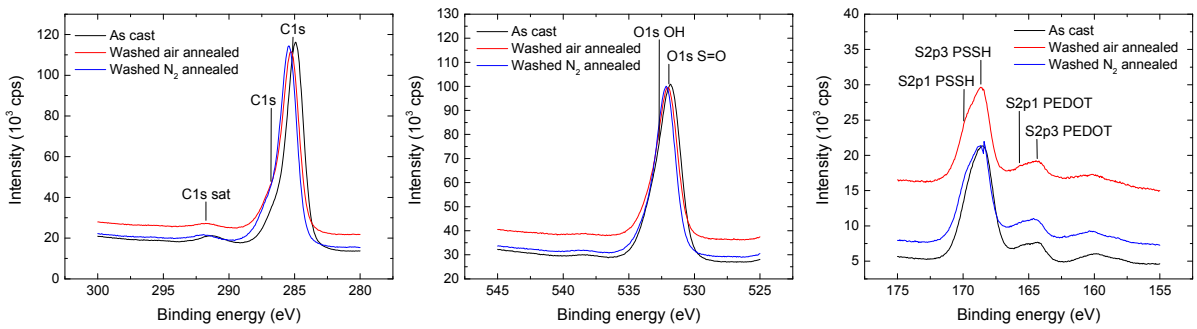

Fig. S14 High resolution XPS spectra of carbon (C), oxygen (O) and sulphur (S) for as cast PEDOT and washed PEDOT layers that had perovskite layers annealed in air (red) and nitrogen (blue) on top of them.

References

1 J. J. Van Franeker, K. H. Hendriks, B. J. Bruijnaers, M. W. G. M. Verhoeven, M. M. Wienk and R. A. J. Janssen, 2016, *Adv. Energy Mater*, 2017, **7**, 1601822

2 H.-H. Fang, R. Raissa, M. Abdu-Aguye, S. Adjokatse, G. R. Blake, J. Even and M. A. Loi, *Adv. Funct. Mater.*, 2015, **25**, 2378–2385.

3 T. Schmidt and K. Lischka, *Phys. Rev. B*, 1992, **45**, 8989–8994.

4 H. A. Klasens, *J. Phys. Chem. Solids*, 1958, **7**, 175–200.

5 X. Wen, Y. Feng, S. Huang, F. Huang, Y.-B. Cheng, M. Green and A. Ho-Baillie, *J. Mater. Chem. C*, 2016, **4**, 793–800.

6 X. Wu, M. T. Trinh, D. Niesner, H. Zhu, Z. Norman, J. S. Owen, O. Yaffe, B. J. Kudisch and X.-Y. Zhu*, J. Am. Chem. Soc.*, 2015, **137**, 2089–2096.